Optics for the 20/20 telescope

H. M. Martin[a], J. R. P. Angel[a], J. H. Burge[a,b], S. M. Miller[a], J. M. Sasian[b] and P. A. Strittmatter[a]

[a]Steward Observatory, University of Arizona, Tucson, AZ 85721
[b]Optical Sciences Center, University of Arizona, Tucson, AZ 85721

ABSTRACT

We present a plan for making the optics of a 21 m telescope that builds on advances in mirror design and fabrication developed for the Large Binocular Telescope (LBT) and other large telescopes. The 21 m telescope, with a fast f/0.7 primary mirror made of only seven large honeycomb-sandwich segments and an adaptive secondary with matching segments, is much stiffer than other designs and offers simpler and more accurate wavefront control. It can be a powerful stand-alone telescope, or one of a pair that move on a circular track to achieve coherent imaging with baselines up to 120 m (the 20/20 telescope). Each segment of the 21 m primary mirror is similar to an 8.4 m LBT primary, and each segment of the 2.1 m adaptive secondary mirror is similar to an LBT secondary. The off-axis segments of both mirrors can be made with the same methods and equipment currently used at the Steward Observatory Mirror Lab, and can be polished with the same stressed-lap polishing system used for the LBT mirrors. A change in algorithm to accommodate the asymmetric surface is required, but no new hardware development is needed because the lap bending is similar to that for the LBT mirrors. Each segment can be measured interferometrically, with a combination reflective and diffractive null corrector producing an accurate aspheric template wavefront and alignment references for the segments.

Keywords: telescopes, optical fabrication, optical testing, aspheres

1. INTRODUCTION

Optical fabrication is a driving factor in the design of telescopes much larger than the current class of 6.5 – 10 m telescopes. Larger telescopes will certainly have segmented primary mirrors, and there is a wide range of options for the size and type of segments. The challenge of optical fabrication has led to telescope designs using spherical segments (OWL[1]) or many hundreds of relatively small segments (OWL and CELT[2]). There are some clear advantages, however, to using segments similar to the 8-m-class mirrors now working in many of the world's most powerful telescopes. All of these telescopes have produced 0.3″ FWHM images in good seeing, and lab measurements demonstrate that the intrinsic image quality of the mirrors is better than 0.015″ FWHM, and 80% in 0.1″ diameter, in green light. There is a great deal of experience in supporting these mirrors and controlling their temperatures in the telescope, with excellent success. Large segments reduce the challenge of maintaining alignment, and 8 m mirrors will produce wavefronts that are smoother over 8 m scales than the wavefronts produced by smaller segments. In the design discussed here, the use of large segments and a segmented adaptive secondary mirror allows adaptive correction for the small discontinuities that do occur at the boundaries of primary segments.

These considerations led us to develop concepts for telescopes based on 8.4 m honeycomb-sandwich segments, the largest mirrors that can currently be made. Two natural geometries are a 21 m telescope with seven segments and a 30-m-class telescope with 19 segments.[3] The mirror technology is mature and has been demonstrated in the MMT and Magellan telescopes, and will soon be in place in the LBT.[4-6] These thick honeycomb sandwich mirrors are stiffer than any other proposed segments and therefore more resistant to the wind forces which will be a major challenge for 20 – 30 m telescopes. Designs for mirror support and thermal control are also mature, and costs are well understood. The adaptive secondary segments are similar to the MMT and LBT adaptive secondaries and will be made with similar techniques.

We favor compact telescopes at the 6.5 m and 8.4 m size because of stiffness and enclosure cost, and these factors are even more important for 20 – 30 m telescopes. Wind-driven aberrations and tracking errors are likely to be a

much greater challenge for larger telescopes than for the current generation. The effects of wind are reduced by minimizing the primary focal length, because a shorter telescope is stiffer and can be better protected from wind. A nearly optimum structure with a lowest resonant frequency of 6.5 Hz is achieved with a 21 m f/0.7 primary mirror, as shown in Figure 1.[7]

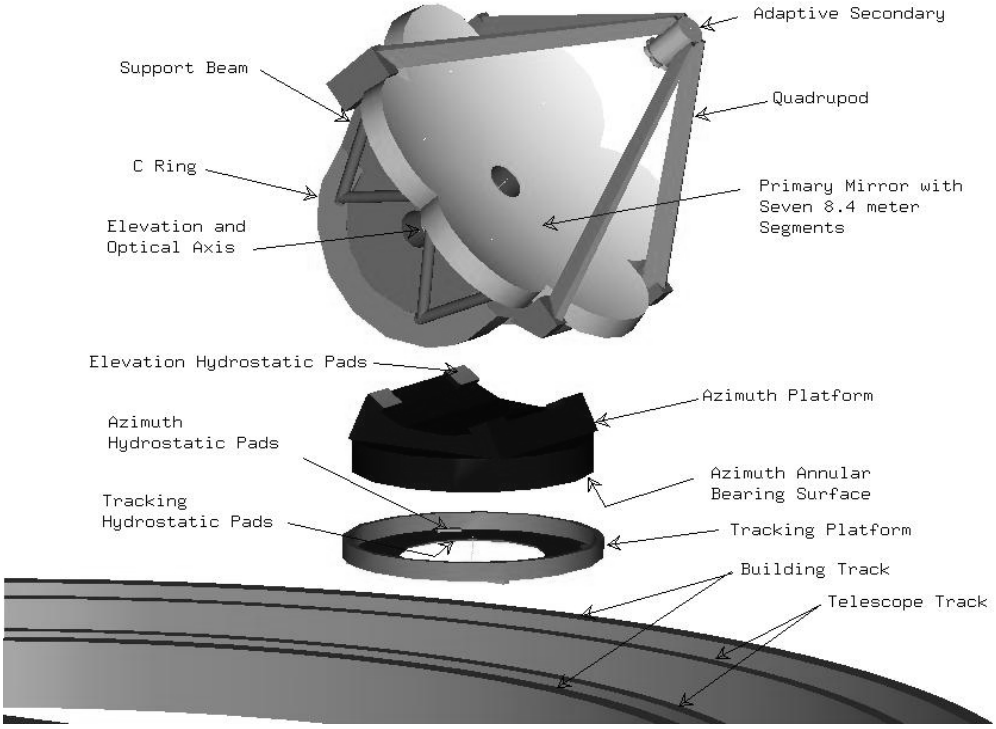

Figure 1. Exploded view of a 21 m telescope, with an f/0.7 primary mirror made of seven 8.4 m segments.

The major drawback of a faster telescope is the increased difficulty of optical fabrication, testing and alignment. In this paper we examine the challenge of fabrication and testing, and show that it represents a very modest step forward from the mirrors we have already made. Little extension of current fabrication techniques is needed, and new testing techniques promise to provide accurate wavefront measurement and initial alignment. Alignment tolerances for lateral translation and rotation of segments are tighter for a fast telescope, but alignment of both the primary and secondary mirror segments in the telescope will be based primarily on wavefront measurements rather than position measurements. Therefore the increased sensitivity to position errors for a fast telescope is irrelevant, provided the hexapod positioning system for each segment has adequate resolution and the structure has adequate stability over the roughly one minute required to average seeing in the wavefront measurement.

A fast 21 m or 30 m telescope with 8.4 m honeycomb-sandwich segments and a segmented adaptive secondary mirror will be a powerful instrument, capable of 3 – 5 mas images. Even higher resolution demands coherent imaging with more than one telescope. The 20/20 telescope represents a class of telescope designs optimized for high-resolution imaging over a wide field of view.[3,8] The pupil geometry is an expanded and flexible version of the LBT, which has two 8.4 m mirrors, separated by 14.4 m center to center, on a common mount. In the LBT, the baseline between mirrors is always perpendicular to the source. The beam combiner preserves the constant pupil geometry, allowing coherent imaging over as wide a field as can be corrected with adaptive optics over each mirror. The baseline rotates through the night, providing 2-dimensional sampling of the *u-v* plane, but its length is fixed. The 20/20 telescope implements the

same pupil geometry by moving two 21 m telescopes separately on a circular track as shown in Figure 2. Light from the two telescopes is brought to a central beam combiner for coherent imaging. The separation between telescopes can be changed in a matter of minutes, allowing full coverage of the *u*-*v* plane out to a baseline of 120 m. Because the telescopes' azimuth tracking is achieved by motion on the track, the compact, stiff structure provided by f/0.7 primary mirrors is especially valuable.

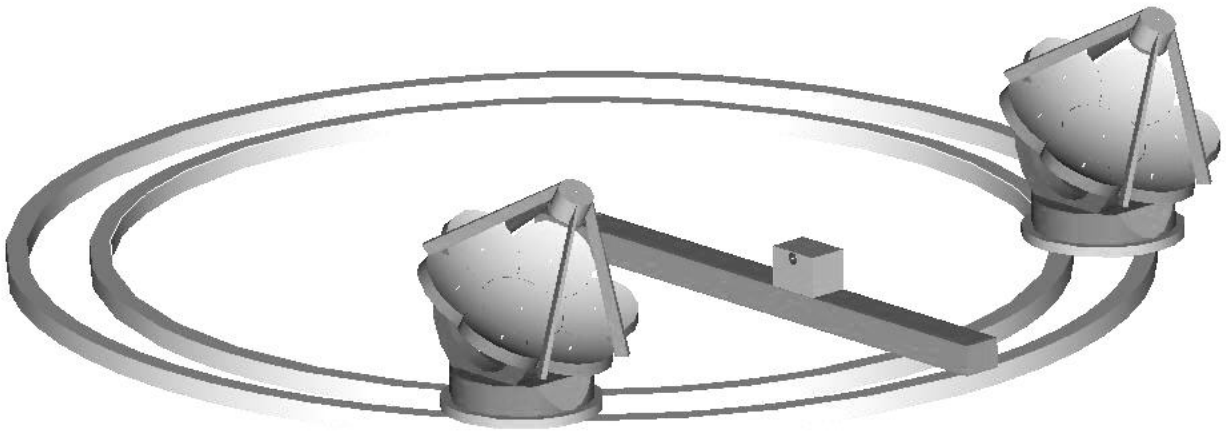

Figure 2. Conceptual drawing of the 20/20 telescope, showing the 21 m telescopes, the central beam combiner, and the 100 m circular track. The pair of telescopes tracks in azimuth only by moving on the track. Compact enclosures (not shown) move on a concentric pair of tracks (also not shown).

One goal that drives the 20/20 design is direct detection of exoplanets through thermal emission or reflected starlight. The telescope will be used as a Bracewell nulling interferometer for this effort. For this and some other scientific goals, high contrast over a field of an arcsecond or more is crucial, and therefore the mirrors must be extremely smooth on scales of centimeters to 1 m. Large segments offer smooth wavefronts over the critical scales, reduce the challenge of maintaining alignment, and minimize diffraction from discontinuities at the boundaries. This is particularly true for the 20/20 design with its adaptive secondary mirrors segmented to match the primary mirrors and therefore capable of correcting inter-segment phase steps.

In this paper we address the optical fabrication and testing of mirrors for a 21 m telescope. Section 2 describes the optical configuration considered. We show in Section 3 that the stressed-lap polishing system used for the MMT and Magellan primaries, and currently being used for the LBT primaries, is capable of achieving smooth and accurate figures on the highly aspheric surfaces of the off-axis segments. We also describe new techniques to measure the figures and achieve accurate alignment of the off-axis segments. Section 4 discusses fabrication and testing of the secondary mirror. Section 5 describes a technology demonstration of off-axis polishing and measurement at the 1.8 m scale. Section 6 outlines a manufacturing plan for the optics of one or two 21 m telescopes.

2. OPTICAL CONFIGURATION

Figure 3 shows the optical configuration for the 21 m telescope considered here. Each segment is part of an 8.4 m diameter mirror, truncated to fit together into a nearly continuous aperture. An alternative configuration uses closely packed circular segments.[3] The honeycomb mirror structure is essentially identical to that of the MMT, Magellan and LBT primary mirrors, as is the mirror support system.

The secondary mirror is segmented in the same pattern at 1/10 scale. The optical surface of the adaptive secondary is a glass shell about 1.6 mm thick, with each of the seven segments controlled by about 800 fast voice-coil actuators. Apart from a small increase in actuator density, the mechanical design is similar to the MMT adaptive

secondary mirror and almost identical to the LBT secondaries.[9] A single stiff glass reference body with a maximum dimension of 2.3 m provides a continuous shape reference for the segmented shell, and allows accurate control of the boundaries at the level of a few nm.

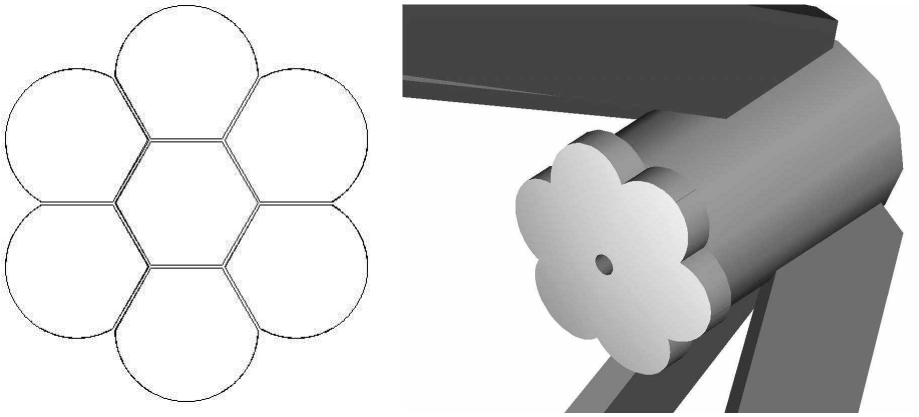

Figure 3. Optical configuration for the 21 m telescope. Primary mirror is made of seven 8.4 m segments, truncated to fit together with minimal gaps as shown at left. Secondary mirror shown at right is identically segmented at 1/10 scale.

Diffraction from the flower-shaped aperture is only slightly more extended than from a circular aperture, as shown in Figure 4. The wings of the point-spread function are dominated by blockage from the secondary mirror support in both cases. Figure 5 shows the effect of combining light from two telescopes coherently. All sources in the adaptively corrected field will have the same PSF, with interference fringes modulating the PSF of the 21 m telescope. The 20/20 or LBT configuration is distinguished from interferometers made from separately mounted telescopes in that the pupil geometry is constant apart from rotation of the baseline. The beam combiner maintains this geometry, which is a condition for wide-field imaging.

3. FABRICATION OF THE PRIMARY MIRROR

Each segment of the 21 m primary mirror has the same maximum diameter as an 8.4 m LBT primary mirror, and essentially the same internal honeycomb structure. In the optical configuration considered here, the central segment is truncated to a hexagon and the six outer segments are truncated to partial hexagons. We can cast these mirrors in the same furnace and a mold similar to that used for the LBT mirrors, which were cast successfully in 1997 and 2000.[6,10] Trimming to hexagons and partial hexagons can be done as part of the mirror casting process, or by cutting the mirrors to the final dimensions at a later stage of processing. In either case, the honeycomb rib pattern would be modified to provide a continuous glass wall along the perimeter of the finished mirror. The overall curvature of the mirror surface is achieved by spinning the furnace while the glass is molten. The 21 m telescope has a focal length of 15 m, longer than the LBT's 9.6 m, so the furnace will spin 25% more slowly. The aspheric departure of the off-axis segments—19 mm peak-to-valley—has little impact on the casting. Even with axisymmetric parabolic primary mirrors, we make no attempt to obtain an accurate surface to better than a few mm, and in fact add about 20 mm of extra glass that will be ground away, to allow for possible leakage during the casting and uncertainty in volume of the complex honeycomb structure.

We will generate the off-axis aspheric surface using the same 8.4 m capacity numerically controlled mill that we use to generate the axisymmetric curves on all large mirrors.[11] For symmetric parabolic mirrors, the generator's diamond-impregnated cutting wheel follows a parabolic path $z(r)$ as the mirror rotates around its axis. For the off-axis segments, the wheel will be given additional radial motion as the mirror rotates around its mechanical axis (not the optical axis) so that the wheel essentially follows contours of constant height on the asymmetric surface.

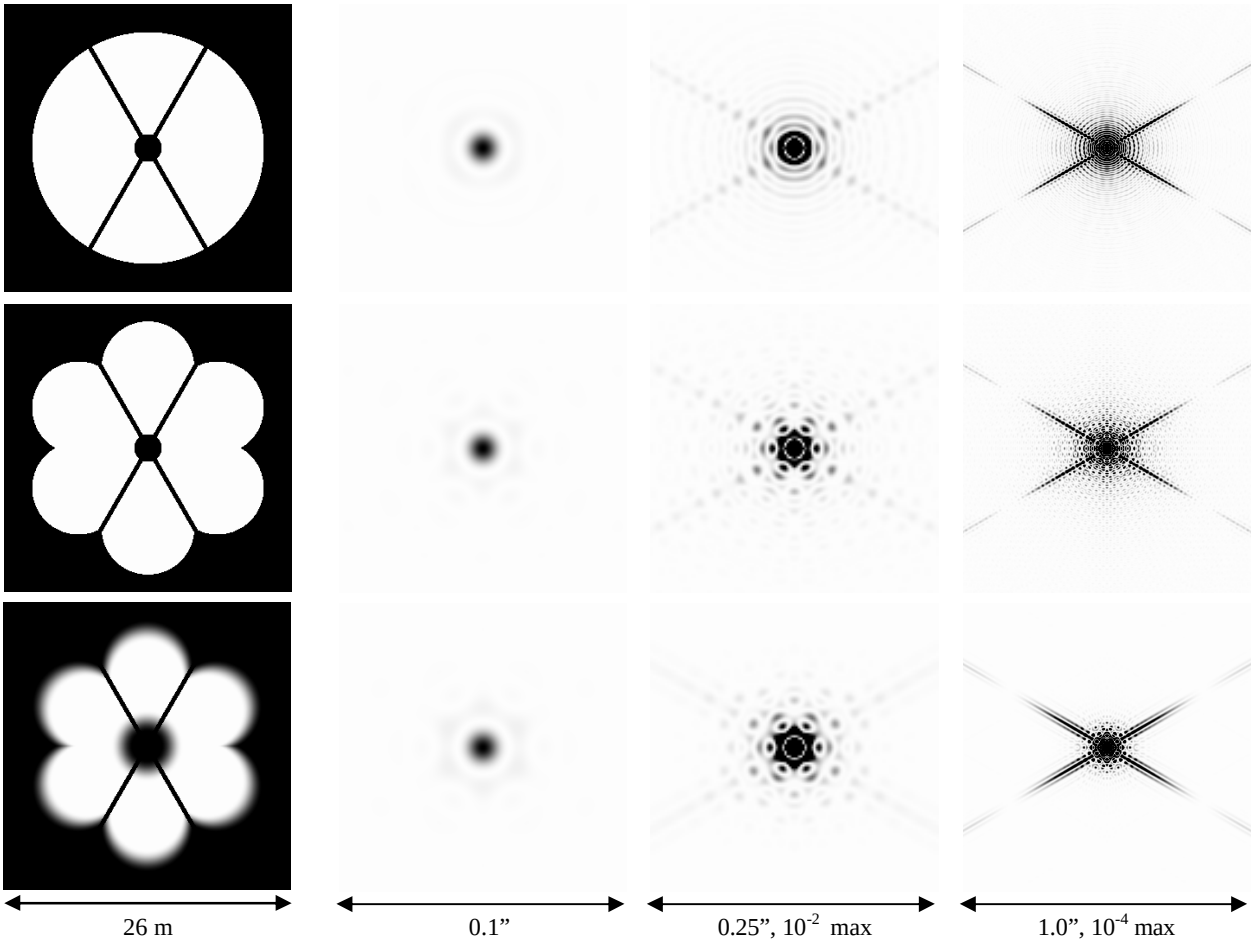

Figure 4. Apertures and point-spread functions for three versions of a 21 m telescope, at a wavelength of 760 nm. From top to bottom: circular aperture; proposed segmented geometry; segmented geometry with cosine apodization over a band 2 m wide at inner and outer edges. Secondary mirror supports are 0.4 m wide. The PSFs are shown at full intensity, clipped at 10^{-2}, and clipped at 10^{-4}.

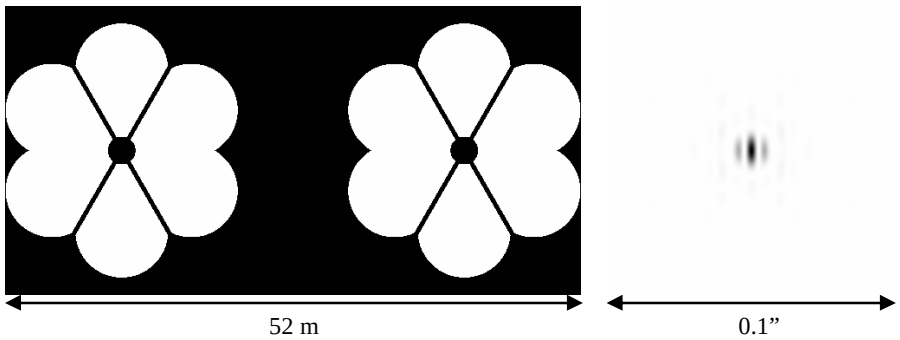

Figure 5. Aperture and point-spread function for the 20/20 telescope with a 31 m baseline, at a wavelength of 760 nm. In this close-packed configuration, the central fringe of the combined PSF contains 50% of the light.

Polishing the off-axis segments presents an interesting challenge. The parent paraboloid that includes the off-axis segments is a 23 m f/0.65. The segments' surfaces depart from the best fitting sphere by 19 mm peak-to-valley, an extraordinary amount in comparison with any large mirror made to date. The aspheric departure is shown in Figure 6. Also shown are the aspheric departures of the symmetric 6.5 m f/1.25 MMT and Magellan primary mirrors that we have polished, and the 8.4 m f/1.14 LBT primaries that we are currently polishing, but amplified by a factor of 10 so they will be visible on the same grayscale used for the off-axis segment. These symmetric mirrors are by far the most aspheric large mirrors ever made—the VLT and Gemini primary mirrors have departures of 0.34 mm peak-to-valley—but they pale in comparison with the segment. Table 1 lists the peak-to-valley asphericity and Zernike polynomial coefficients for all significant components. Asphericity is generally taken as a measure of the difficulty of polishing and measuring a mirror. In polishing, it is difficult to keep the tool, or lap, in intimate contact with an optical surface whose curvature changes from point to point. In testing, it is difficult to produce an accurate template wavefront for an aspheric surface.

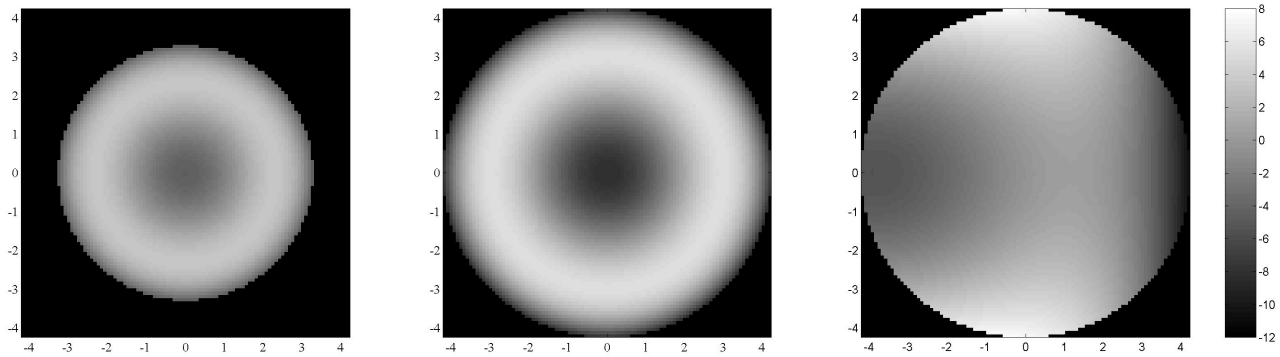

Figure 6. Aspheric departure of (left to right) 6.5 m f/1.25 mirror, 8.4 m f/1.14 mirror, 8.4 m segment centered 7.3 m off the axis of a 23 m f/0.65 parent. Axes are labeled in m and gray bar is labeled in mm (20 mm peak-to-valley). Aspheric departures of the symmetric 6.5 m and 8.4 m mirrors are amplified by a factor of 10 to make them visible on the same grayscale used for the off-axis segment. The real amplitudes of asphericity are listed in Table 1. The aspheric departure for the segment is plotted over a full 8.4 m circle although the aperture may be truncated as in Figure 3.

Table 1. Peak-to-valley aspheric departure and Zernike polynomial coefficients of mirrors shown in Figure 6. Units are mm and Zernike polynomials are normalized to unity at the edge of the mirror.

	6.5 m f/1.25	8.4 m f/1.14	8.4 m segment of 23 m f/0.65
peak-to-valley	0.81	1.38	18.69
astigmatism	0	0	-7.92
coma	0	0	-2.85
spherical aberration	-0.54	-0.92	-0.21

The polishing system developed at the Steward Observatory Mirror Lab was designed specifically for highly aspheric mirrors such as the MMT, Magellan and LBT primaries.[12] At the heart of the process is a polishing tool, shown in Figure 7, that changes shape continuously as it moves across the mirror, so it always matches the local shape of the mirror surface. The tool, called a stressed lap, is stiff enough to provide strong passive smoothing of unwanted structure, but is bent elastically by a set of actuators under computer control. For symmetric parabolic mirrors, the lap has a symmetric shape when it is over the center of the mirror, and distorts into an off-axis paraboloid as the polishing motion moves it off axis. The same process works for an off-axis mirror segment; the only difference is that the lap never visits

the center of the parent paraboloid. This polishing system thus has no fundamental preference for symmetric mirrors over off-axis mirrors; the lap can be programmed to follow the local surface shape in either case.

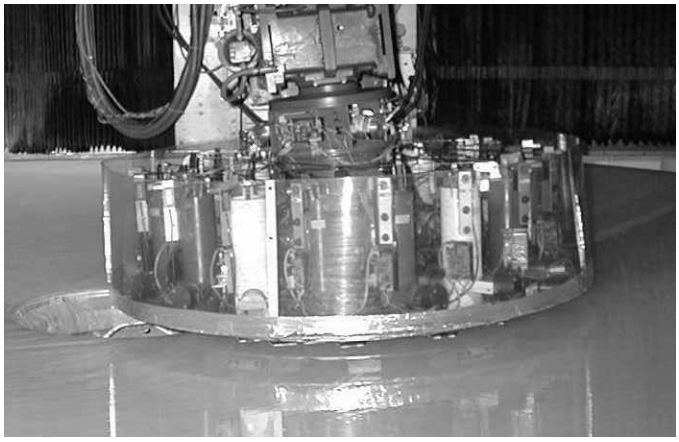

Figure 7. 1.2 m diameter stressed lap polishing tool, shown polishing a 6.5 m f/1.25 mirror.

The ultimate limit to the polishing system employed at the Mirror Lab is the amount of bending that can be achieved accurately. The amount of bending required depends on the curvature variations across the mirror. The curvature variations are related to asphericity but depend on the precise shape of the aspheric departure. As shown in Table 1, most of the asphericity in the off-axis segment is in the form of astigmatism and coma, aberrations that involve relatively small changes in curvature. For the symmetric parabolic mirrors, the asphericity has the form of Seidel spherical aberration, which has relatively strong changes in curvature. In fact, the off-axis segment has four times less spherical aberration than the LBT primary.

Imagine the 1.2 m diameter stressed lap moving across the mirror surfaces in Figure 6, bending to match the local shape. Figure 8 shows the maximum shape change the lap experiences, and Table 2 lists the peak-to-valley shape change and Zernike polynomial coefficients. Remarkably, the lap bends less than twice as much for the off-axis segment as for the symmetric 6.5 m and 8.4 m mirrors, despite the fact that the segment has 13 times the asphericity of the LBT mirror. The overall asphericity of the larger and faster mirror is much greater, but its curvature variations are only slightly greater. Not only is the required lap bending surprisingly small, but it is easily induced in the lap plate. Figure 9 shows the bending moment needed to bend the stressed lap, for the symmetric mirrors and the off-axis segment. The range of moments around the lap plate is slightly *less* for the segment than for the MMT/Magellan mirror. The reason is that the curvature variations across the lap are less for the off-axis segment. The lap bending for the segment is almost entirely focus (axisymmetric bending) and astigmatism, both relatively flexible bending modes with constant curvature. The lap bending for MMT/Magellan and LBT contains more coma, a much stiffer mode because of its linear variation of curvature across the lap.

Another way of looking at the curvature variations is to consider the derivative of curvature with respect to position on the mirror. The aspheric departure of a parabolic mirror of diameter $D = 2r_m$ and radius of curvature R is

$$z = \frac{1}{48R^3}(6r^4 - 6r_m^2 r^2 + r_m^4),$$

where r is the radial coordinate on the surface. The peak-to-valley aspheric departure is $\frac{D}{4096 f^3}$, where $f = \frac{R}{2D}$ is the focal ratio. The derivative of curvature is a third derivative of the aspheric departure, so depends strongly and

inversely on diameter; its maximum value (at the edge of the mirror) is $\frac{3}{16} f^{-3} D^{-2}$. While the asphericity increases for larger or faster mirrors, a mirror that is larger *and* faster may have curvature variations similar to or even less than those of a smaller, slower mirror. It is the curvature variation that determines the difficulty of figuring. Curvature variations are critical to all lapping processes—not only stressed-lap polishing—so the implication is that telescopes of 20-50 m diameter can be much faster than 8 m class telescopes without increasing the difficulty of polishing.[13]

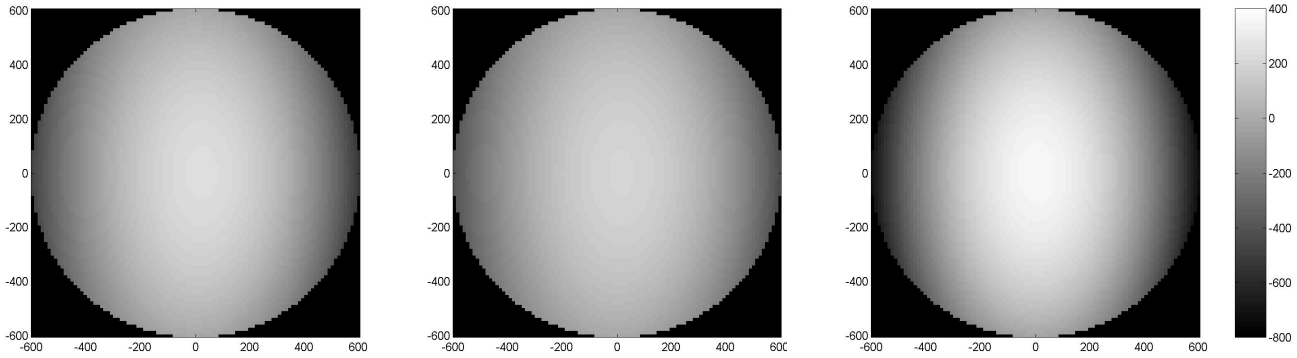

Figure 8. Change in lap shape for a 1.2 m stressed lap used to polish the three mirrors of Figure 6. The quantity plotted is the difference between lap shape at the edge of the mirror and shape at the center of the mirror (or parent). From left to right, 6.5 m f/1.25 mirror, 8.4 m f/1.14 mirror, 8.4 m segment centered 7.3 m off the axis of a 23 m f/0.65 mirror. Axes are labeled in mm and gray bar is labeled in μm (1200 μm peak-to-valley). All plots have the same grayscale.

Table 2. Peak-to-valley deformation and Zernike polynomial coefficients for a 1.2 m stressed lap used to polish the mirrors of Figure 6. Units are μm and Zernike polynomials are normalized to unity at the edge of the mirror.

	6.5 m f/1.25	8.4 m f/1.14	8.4 m segment of 23 m f/0.65
peak-to-valley	657	654	1125
focus	-212	-213	-377
astigmatism	-209	-209	-358
coma	-24	-19	-11

Polishing the mirror is only part of the challenge. Measuring an off-axis segment of a very fast parent also requires innovations in two areas. The first is measurement of the asymmetric aspheric surface to an accuracy about six orders of magnitude smaller than its asphericity. This measurement requires a template wavefront of the same shape as the desired surface, and the accuracy of the measurement is no better than the accuracy of the template. For an aspheric surface, the template is formed by a null corrector, generally a set of lenses, mirrors or both that converts a spherical or planar wavefront to the desired aspheric shape. For the LBT primary mirror, the null corrector comprises two lenses, the larger being 290 mm in diameter and 74 mm thick. The goal for this null corrector is to add 1.4 mm peak-to-valley spherical aberration to the initial spherical wavefront, to an accuracy of 140 nm in the dominant aberration and 50 nm rms in the residual error.[14,15] A traditional null corrector aims to achieve an almost perfect wavefront, such that the residual errors can be ignored, with a single set of elements, either transmissive, reflective or diffractive. A system of this type for the segment of a 23 m f/0.65 parent would be so large that it cannot be built to the required accuracy. A practical solution is a two-stage null corrector, where the first stage (transmissive or reflective) creates a wavefront with

the correct low-order shape, and the second stage (diffractive) corrects the residual error. An example of the first stage of such a system for the off-axis segment is shown in Figure 10. Two spherical mirrors no more than 1 m in diameter and separated by 3.2 m make the low-order compensation. A computer-generated hologram corrects the residual error.[13]

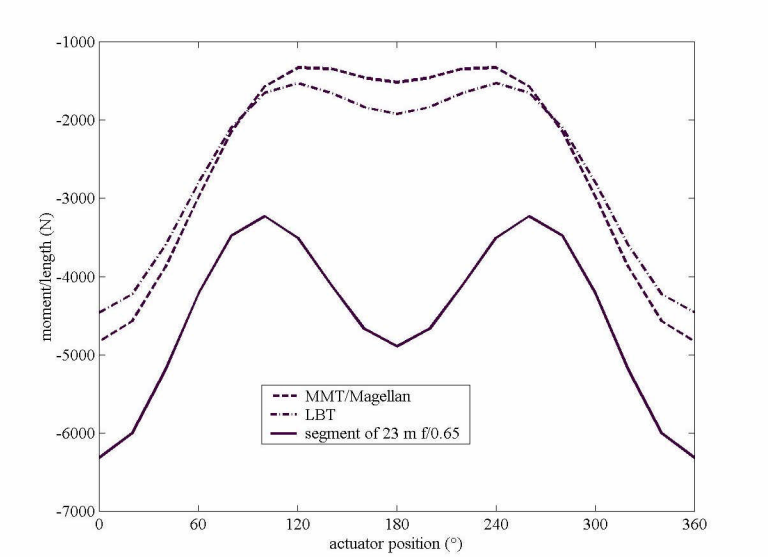

Figure 9. Moments required to bend the stressed lap, for the three mirrors of Figure 6. The quantity plotted is the bending moment per unit length around the circumference of the plate. The scaling depends on the lap plate's material and dimensions; this is for a 1.2 m diameter, 50 mm thick, aluminum plate. A constant moment, independent of actuator position, induces axisymmetric bending, so the offset between graphs would be eliminated by choice of the curvature of the polishing surface for the unstressed plate. Only the range of the graphs is important.

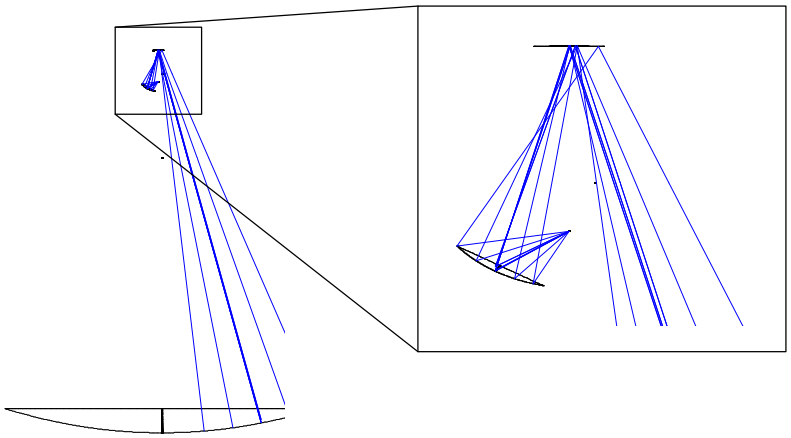

Figure 10. Reflective null corrector that makes a low-order compensation for the 19 mm aspheric departure of a 20/20 segment. Located near the center of curvature 30 m above the segment, the null corrector comprises two spherical mirrors separated by 3.2 m. The full parent paraboloid is shown at left, but only one segment is measured at a time. A computer-generated hologram (not shown) compensates the residual high-order asphericity.

The second challenge for the measurement system is aligning the segments. For the segmented f/0.7 primary mirror, we must know the relation between the optical axis and each segment's mechanical axis to high accuracy.[13] This

can be achieved with the same hologram that corrects the wavefront as the second stage of the null test. Burge[16] has designed holograms containing multiple patterns, including

1. wavefront correction (second stage of the null corrector);
2. creation of wavefronts that return to the interferometer for alignment of the test;
3. creation of crosshair images at different locations for alignment of segments relative to the optical axis of the parent and to each other.

All patterns are written at once using electron beam lithography, so the registration between them is excellent. The crosshair patterns will determine the segment's position relative to the optical axis and its neighbors to sub-mm accuracy.

4. SECONDARY MIRROR FABRICATION

The secondary mirror of the 21 m telescope is segmented to match the primary, with seven segments covering an area whose maximum dimension is 2.3 m. It is also adaptive, consisting of thin glass shells supported by about 5400 actuators (800 in each outer segment). We have developed a process for manufacturing the thin shells through a series of prototypes and the MMT adaptive secondary.[17] Polishing the segments is challenging because of their severe asphericity as well as their flexibility. We care little about the large-scale figure because it will be determined entirely by the actuators, but we must achieve a smoothness on the order of 10 nm rms surface error on scales too small to be corrected by the actuators. The stressed-lap polishing system is an excellent method of achieving the small-scale smoothness on the aspheric surface, but it applies large polishing forces and is best for stiff mirrors. In an earlier process used for the MMT adaptive secondary shell, we polished the mirror at its final 2 mm thickness by bonding it to a rigid glass "blocking body" with a thin layer of pitch. This method was a qualified success, leaving figure errors due to uneven pressure in the pitch bond layer over the rear surface of the shell. For the LBT secondaries, we will figure the optical surfaces on thick mirror blanks, then thin them to the final thickness of 1.6 mm by grinding the rear surfaces. The thinning process will cause the optical surface to deform with the removal of several cm of glass and its internal stress, but the deformations should be on sufficiently large scales that they will be corrected by the actuators with modest forces.

For the secondary of the 21 m telescope, it may be easier to figure the 2.3 m mirror as one piece, then cut it into segments after thinning it. A full-aperture measurement of the convex asphere could also be set up, using techniques already demonstrated with the 1.7 m f/5 secondary for the MMT. We measure the figure in the early stages mechanically with a swing-arm profilometer that makes one-dimensional traces accurate to 50 nm rms surface. The final measurements are full-aperture interferometric tests made using a holographic test plate.[18] Figuring and supporting a 1.7 m test plate proved to be difficult, as did the 2.5 m illumination system that brings light in normal to the surface of the secondary. We therefore favor a subaperture test—essentially one segment at a time—for the secondary of the 21 m telescope. Like the test of primary segments, this is a two-stage null test, illustrated in Figure 11. The two spherical mirrors shown put the low-order asphericity into the test wavefront, while a computer-generated hologram corrects the residual error and projects alignment reference marks onto the secondary mirror.

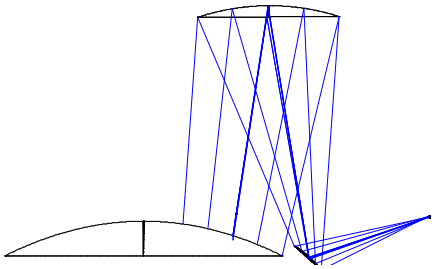

Figure 11. Reflective null corrector that makes a low-order compensation for the asphericity of a segment of the secondary mirror. The full 2.3 m secondary is shown but only one segment is measured at a time. A computer-generated hologram (not shown) compensates the residual high-order asphericity.

5. DEMONSTRATION OF OFF-AXIS FIGURING AND MEASUREMENT

We plan to demonstrate and refine the techniques described here by making a 1.8 m off-axis segment of a 7 m f/0.7 parent paraboloid. This is roughly a 1/4 model of a primary mirror segment for the 21 m telescope, although the geometry is constrained by the diameter and focal length of an existing mirror. The demonstration will use our 2 m stressed-lap polishing machine, generally used for secondary mirrors, and a 1.8 m f/2.7 lightweighted mirror. The polishing machine has a 30 cm diameter stressed lap. Like the 1.2 m lap analyzed in Section 3, this lap can bend to follow the 3 mm peak-to-valley asphericity of the 1.8 m segment. We will use the new holographic testing and alignment techniques described in Section 3. For comparison, we can measure the off-axis parabolic mirror with a straightforward autocollimation test using a 1.8 m flat mirror, a test geometry that would be prohibitively expensive for an 8.4 m segment.

6. MANUFACTURING PLAN

8.4 m segments made at the Mirror Lab would follow the standard sequence for 8.4 m honeycomb sandwich mirrors: casting, generating and polishing. The steps would be modified in several ways as described in Section 3. Each step takes about the same amount of time, which has been reduced from over a year to about 9 months for the mirrors currently being processed. (The generating step includes the time required to polish the rear surface and bond loadspreaders that will interface with the support system.) The Mirror Lab currently has one 8.4 m capacity machine for generating and polishing, so it forms a bottleneck in the production cycle. A second machine is being built by In-Place Machining to be installed in early 2003; it will be used exclusively for polishing while the original machine will revert to being a generator. With this equipment in place, we project that 8.4 m mirrors will be produced at 9 month intervals, with the first mirror completed about 27 months after the beginning of the project. This projection assumes that the added technical challenge of the off-axis segments is balanced by improved efficiency in mass production. Thus a 21 m primary mirror made of seven segments plus one spare would be finished in about 7.5 years.

Making two 21 m primary mirrors (14 segments plus one spare) in the Mirror Lab facility would take 12-13 years, which is unacceptably long. The full 20/20 optics would require a second facility with the same capabilities in casting, generating, polishing and measurement. It could be obtained by duplicating the Mirror Lab or by enhancing an existing facility.

7. CONCLUSION

We have described a plan for manufacturing 21 m primary mirrors made of 8.4 m segments, and 2.1 m adaptive secondary mirrors with matching segmentation. Production of mirror blanks, generating, and polishing the mirrors to high accuracy can be done with existing techniques and equipment. We have developed promising techniques for measurement and alignment of the primary and secondary mirror segments, and will demonstrate these techniques on a 1.8 m scale in the near future. We have analyzed the full manufacturing process and found no significant technical barriers. Experience with three 6.5 m and two 8.4 m mirrors shows that the Mirror Lab could produce a 21 m primary mirror in about 7.5 years, while the Mirror Lab plus a similar additional facility could produce two 21 m primary mirrors in the same time.

REFERENCES

1. P. Dierickx, R. Gilmozzi, “Progress of the OWL 100-m Telescope Conceptual Design”, in *Telescope Structures, Enclosures, Controls, Assembly/Integration/Validation, and Commissioning*, ed. T. Sebring, T. Andersen, Proc. SPIE 4004, p. 290 (2000).
2. J. E. Nelson, “Design Concepts for the California Extremely Large Telescope (CELT)”, in *Telescope Structures, Enclosures, Controls, Assembly/Integration/Validation, and Commissioning*, ed. T. Sebring, T. Andersen, Proc. SPIE 4004, p. 282 (2000).

3. R. Angel, J. Burge, J. Codona, W. Davison, B. Martin, “20 and 30 m telescope designs with potential for subsequent incorporation into a track-mounted pair (20/20 or 30/30)”, in these proceedings.
4. S. C. West, S. Callahan, F. H. Chaffee, W. B. Davison, S. T. DeRigne, D. G. Fabricant, C. B. Foltz, J. M. Hill, R. H. Nagel, A. D. Poyner, J. T. Williams, “Toward first light for the 6.5-m MMT telescope”, in *Optical Telescopes of Today and Tomorrow: Following in the Direction of Tycho Brahe*, ed. A. Ardeberg, Proc. SPIE 2871, p. 38 (1997).
5. S. A. Shectman, “The Magellan Project”, in *Telescope Structures, Enclosures, Controls, Assembly/Integration/Validation, and Commissioning*, ed. T. Sebring, T. Andersen, Proc. SPIE 4004, p. 47 (2000).
6. J. M. Hill, P. Salinari, “The Large Binocular Telescope Project, in *Telescope Structures, Enclosures, Controls, Assembly/Integration/Validation, and Commissioning*, ed. T. Sebring, T. Andersen, Proc. SPIE 4004, p. 36 (2000).
7. W. Davison, N. Woolf, R. Angel, “Design and analysis of 20 m track-mounted and 30 m telescopes”, in these proceedings.
8. R. Angel, M. Lloyd-Hart, K. Hege, R. Sarlot, C. Peng, “The 20/20 telescope: MCAO imaging at the individual and combined foci”, in *Beyond Conventional Adaptive Optics*, ESO Conference Proc., ed. R. Ragazzoni, S. Esposito (2001).
9. M. Lloyd-Hart, F. Wildi, H. Martin, P. McGuire, M. Kenworthy, R. Johnson, B. Fitz-Patrick, G. Angeli, S. Miller, and R. Angel, “Adaptive optics at the 6.5 m MMT”, in *Adaptive Optical Systems Technology*, ed. P. L. Wizinowich, Proc. SPIE 4007, p. 167 (2000).
10. B. H. Olbert, J. R. P. Angel, J. M. Hill, S. F. Hinman, “Casting 6.5-meter mirrors for the MMT conversion and Magellan”, in *Advanced Technology Optical Telescopes V*, ed. L. M. Stepp, Proc. SPIE 2199, p. 144 (1994).
11. D. A. Ketelsen, W. B. Davison, S. T. DeRigne, W. C. Kittrell, “Machine for complete fabrication of 8-m class mirrors”, in *Advanced Technology Optical Telescopes V*, ed. L. M. Stepp, Proc. SPIE 2199, p. 651 (1994).
12. H. M. Martin, R. G. Allen, B. Cuerden, S. T. DeRigne, L. R. Dettmann, D. A. Ketelsen, S. M. Miller, G. Parodi and S. Warner, “Primary mirror system for the first Magellan telescope”, in *Optical Design, Materials, Fabrication, and Maintenance*, ed. P. Dierickx, Proc. SPIE 4003, p. 2 (2000).
13. J. H. Burge, H. M. Martin, “Optical issues for giant telescopes with extremely fast primary mirrors”, in these proceedings.
14. J. H. Burge, D. S. Anderson, D. A. Ketelsen, S. C. West, “Null test optics for the MMT and Magellan 6.5-m f/1.25 primary mirrors”, in *Advanced Technology Optical Telescopes V*, ed. L. M. Stepp, Proc. SPIE 2199, p. 658 (1994).
15. J. M. Sasian, S. A. Lerner, J. H. Burge and H. M. Martin, “Design, tolerancing, and certification of a null corrector to test 8.4-m mirrors”, in *Optical Fabrication and Testing*, ed. R. Geyl, Proc. SPIE 3739, p. 444 (1999).
16. J. Burge, P. Koudelka, “Optical test alignment using computer generated holograms”, in *Optical Fabrication & Testing*, OSA Technical Digest, p. 105 (2001).
17. H. M. Martin, J. H. Burge, C. Del Vecchio, L. R. Dettmann, S. M. Miller, B. Smith and F. Wildi, “Optical fabrication of the MMT adaptive secondary mirror”, in *Adaptive Optical Systems Technology*, ed. P. L. Wizinowich, Proc. SPIE 4007, p. 502 (2000).
18. J. H. Burge, “Measurement of large convex aspheres”, in *Optical Telescopes of Today and Tomorrow: Following in the Direction of Tycho Brahe*, ed. A. Ardeberg, Proc. SPIE 2871, p. 362 (1997).